Resistivity and magnetoresistivity measurements near the metal-insulator and superconductor-insulator transition in granular Al-Ge

G. Eytan and R. Rosenbaum
School of Physics and Astronomy, Tel Aviv University, Raymond and Beverly Sackler Faculty of Exact Sciences, Ramat Aviv 69978, Israel

D. S. McLachlan and A. Albers
Physics Department and Condensed Matter Physics Research Unit, University of the Witwatersrand, P.O. Wits, 2050, Johannesburg, South Africa

(Received 11 December 1992; revised manuscript received 19 April 1993)

Granular Al-Ge films just on the metallic side of the critical volume fraction ϕ_c (50.7% Al) are found to have critical fields in excess of 1.5 T at 0.47 K due to the fine granular nature of the Al. In barely insulating films where $(\phi_c-\phi)<2.2\%$ (where ϕ is the volume percent of aluminum), superconducting fluctuations and Josephson-junction coupling dominate the behavior below T_c ($T_c\simeq 1.6$ K). For the more insulating films where $3.4\%\leq(\phi_c-\phi)\leq 6.2\%$, the resistivity diverges strongly below T_c and a large negative magnetoresistivity is observed. This behavior is explained in terms of quasiparticle tunneling or alternatively by the Adkins charging model; the magnetoresistivity is explained in terms of a magnetic-field-dependent superconducting energy gap. The upper critical fields of all the samples are found to be almost independent of the bulk resistivities, supporting a picture of weakly coupled grains. The normal resistivity in the insulating films ($\phi<\phi_c$) obeys the hopping relation $\rho=\rho_0\exp(T_0/T)^x$ above T_c and also below T_c in a field of 3.48 T, which quenches all superconductivity in the films.

I. INTRODUCTION

There has been a long and sustained interest in the resistivity and superconductivity, as well as the metal-insulator and superconductor-insulator transitions, in granular metal films and other disordered systems. The resistivity and, less often, the magnetoresistivity have been studied over a large range of the relative volume fractions of the two components of the granular composite or cermet and also over a wide range of temperatures. Unfortunately, all of these measurements are seldom made on the same systems. Metal-insulator and superconductor-insulator studies naturally concentrate on measurements near the critical volume fraction. An extensive and still basic review on the above was written by Abeles in 1976.[1] In 1983 these properties as related to percolation theory, in granular Al-Ge and other systems, were reviewed by Deutscher, Kapitulnik, and Rappaport.[2] A comprehensive study of both the volume fraction and temperature dependence of the resistivity in the Al-Ge system has recently been completed by McLachlan *et al.*,[3] and the thermoelectric power was measured and explained by Hurvits, Rosenbaum, and McLachlan.[4] These two articles and the present one together constitute the most thorough investigation of the granular Al-Ge system yet made.

This paper focuses on the resistivity and magnetoresistivity close to the metal-insulator and superconductor-insulator transitions in the granular Al-Ge system that occur at or near the percolation threshold for the Al grains. Also examined in this paper is the variation of the parameters T_0 and x, obtained from the general hopping resistivity equation $\rho=\rho_0\exp(T_0/T)^x$, on the insulating side of the metal-insulator transition. Other two- and three-dimensional (3D) systems in which similar studies have been made include pressed oxidized In, Sn, and Pb submicron particles[5] (3D), granular Sn and Pb films[6,7] (2D), granular In (2D) and polysulphurnitride[8] (1D), granular Al-Al_2O_3 (Refs. 9 and 10) (3D), granular In-InO_x (Refs. 11 and 12) (3D), and ultrathin granular metal films.[13]

As the observed resistivity and magnetoresistivity cover a near infinite range in resistivity, many different resistivity and magnetoresistivity mechanisms must be used to explain the results. Therefore, the theory section presents some of the ideas and equations which are used to interpret the wide range of experimental results. Section III gives the experimental method, Sec. IV presents and discusses the results, and Sec. V gives the conclusions.

II. THEORY

Although some of the theoretical models and equations will be introduced at the appropriate place in the results section, many of the equations and the ideas behind them are too detailed to be introduced in the discussion without a major digression. Therefore, these equations and ideas are introduced in this section.

A. Hopping conductivity

The region where the sample consists of isolated grains or granular clusters, and where hopping conductivity

occurs between them, is known as the dielectric region.[1] Historically the first model is that of Neugebauer and Webb[14] in which transfer of electrons between neighboring metal grains is by tunneling, thermal activation being required to provide the non-negligible electrostatic energy that is associated with placing an electronic charge on a grain, creating a "carrier." At low temperatures, the conductivity should behave as[14]

$$\sigma=\sigma_0\exp[-2s/\xi-E_c^0/(k_BT)] , \tag{1}$$

and a simple thermal activation temperature dependence should be observed. In Eq. (1) ξ is the localization length, s is the separation between metallic islands, and E_c^0 is the island charging energy, given by

$$E_c^0=2e^2/\epsilon d , \tag{2}$$

where ϵ is the dielectric constant of the insulator and d the typical diameter of a "spherical" metal grain.

However, using a model where the ratio of s to d is only a function of the metal volume fraction, Sheng, Abeles, and Arie predicted a conductivity whose temperature variation is given by[15]

$$\sigma(T)=\sigma_0\exp[-2(\chi sE_c^0/k_BT)^{1/2}] . \tag{3}$$

Here $\chi=[2m\varphi/\hbar^2]^{1/2}$, where φ is the barrier height. This form of the temperature dependence is very often observed.[1] Note that the above two models involve hopping only between nearest neighbors.

Adkins has made a detailed analysis of transport in granular systems by critical path methods (which is similar to effective medium theory in these systems), incorporating realistic distributions of s and E_c^0, and finds a temperature dependence which is still very close to simple activation.[16]

There are a number of variable-range-hopping mechanisms all of which give rise to the following conductivity formula:

$$\sigma(T)=\sigma_0\exp[-(T_0/T)^x] , \tag{4}$$

where k_BT_0 (a characteristic energy) and x (the exponent) both depend on the particular model. In Mott's classical variable-range-hopping formula, $x=\frac{1}{4}$ for noninteracting particles in 3D.[17] In general,[18]

$$x=(p+1)/(D+p+1) . \tag{5}$$

Here D is the dimension and p the index with which the density of states is assumed to vary about the Fermi energy, i.e., $N(E)=N(O)E^p$. As Mott assumed a constant density of states ($p=0$) this gives $x=\frac{1}{4}$ in three dimensions.[17] Efros and Shklovskii's Coulomb gap model gives $p=2$ and, $x=\frac{1}{2}$ in three dimensions.[19] However, Adkins showed that there are serious inconsistencies in applying the Coulomb gap model to various granular dielectric systems where $x=\frac{1}{2}$ is widely observed.[18,20]

Sheng,[21] starting from the original model for variable range hopping, showed that the factor of $\frac{1}{4}$, derived by Mott,[17] can become $\frac{1}{2}$ in a convolution of a log-normal distribution of the sizes (energies) of the particles with the smearing effect of random potentials. Sheng now also confirms that, for nearest-neighbor hopping, $x=1$.[21]

The variable-range-hopping models all involve an effective dielectric constant. If the electron tunnels between non-neighboring grains, the dielectric constant involved in all these formulas is then some effective average between the dielectric constant of the conducting grains (nearly infinite) and the insulator, which depends both the microstructure and the variable distance between the grains involved in the tunneling process. Percolation theory,[22] Bruggeman's symmetric effective media equation, dynamic scaling theory,[23] and the general effective media equation[24,25] predict a divergent or nearly divergent macroscopic dielectric constant as the metal-insulator transition or percolation threshold is approached from the insulating side. The exact value of ϵ to use in variable range hopping is therefore not clear, but it can obviously change drastically with composition, especially near the percolation threshold.

The conclusion of this section is that while granular samples can, at low enough temperatures, have a temperature dependence given by Eq. (4), T_0 and x depend on the composition and microstructure and may also vary with temperature. It is also clear that a knowledge of T_0 and x is not always sufficient to identify the specific conduction mechanism and that situations intermediate between the theoretically accepted and often observed values of x ($\frac{1}{4}$, $\frac{1}{2}$, 1 in three dimensions) can exist.

B. Quasiparticle tunneling in the superconducting state

To account for the temperature dependence of the resistivity, below the superconducting transition temperature of aluminum in certain samples where quasiparticle tunneling is the dominant mechanism, the following expression for the quasiparticle tunneling current I_{ss} between identical superconductors in the planar configuration should be considered:[26,27]

$$I_{ss}=\frac{2G_n}{e}e^{-\Delta_0/k_BT}\left[\frac{2\Delta_0}{eV+2\Delta_0}\right]^{1/2}(eV+\Delta_0)\times\left[\sin\frac{eV}{2k_BT}\right]K_0\left[\frac{eV}{2k_BT}\right] . \tag{6}$$

Here G_n is the normal junction conductance, Δ_0 the temperature- (and field-) dependent BCS gap, V the voltage across the junction, and K_0 the zeroth-order modified Bessel function. The equation holds for $k_BT\ll\Delta_0$ and $eV<2\Delta_0$. However, it can be shown that, in our situation, eV is of the order of 1–10 μeV per junction, $eV\ll k_BT$ over the experimental temperature range, and $eV\ll\Delta_0$, except when the junction is very close to the transition temperature. In these limits I_{ss} goes to zero as $\sinh(z)K_0(z)$ or $-z\ln(z)$, where $z=eV/2k_BT$.[28] Neglecting the weak log divergence compared with the linear approach to zero, one gets the constant superconducting conductance ($G_{ss}=I_{ss}/V$) that is to be expected at very small voltages. The ratio of G_n/G_{ss} is then given by

$$G_n/G_{ss}=\rho_{ss}/\rho_n=\exp[\Delta_0(T,H)/k_BT]/[\Delta_0(T,H)/k_BT] . \tag{7}$$

While this expression may be correct for $k_B T < \Delta_0$, it obviously diverges at T_c where Δ_0 tends to zero but where ρ_{ss}/ρ_n should tend to one. The temperature dependence of our experimental data is therefore fitted to the semiphenomenological expression

$$\rho_{ss}/\rho_{nn} = \{1 - 1/[\Delta_0(0,0)/k_B T_c]\} + \exp[\Delta_0(T,0)/k_B T]/[\Delta_0(0,0)/k_B T] \ . \quad (8)$$

This expression should be a very good approximation for $T < T_c/2$ where the gap is very close to $\Delta_0(0,0)$ and the exponential expression is large compared to one. The first term ensures that the expression equals one at T_c and that both limits of Eq. (8) are correct. It must be emphasized that Eq. (6) is derived for tunneling between two larger planar electrodes, each of which has a constant chemical potential and a small potential difference between them. Changes in the charging energy, as a thermally activated electron tunnels from a charged to a neutral grain, are certainly not taken into account in Eq. (6).

However, it is found that the results in this paper can be better fitted to an equation of the form

$$\rho_{ss}/\rho_n = (1 - A) + A \exp[\Delta_0(T,H)/k_B T] \ , \quad (9)$$

which has even less physical foundation than Eq. (8). However, the form of Eq. (8), which is dominated by the exponential, to some extent justifies Eq. (9).

C. Adkins variable range quasiparticle hopping model

This section is an abbreviated version of the theoretical discussion presented by Kim, Kim, and Lee[12] on the model, first due to Adkins, Thomas, and Young.[8] Adkins, Thomas, and Young have shown that the charge transfer rate from an initially charged grain to a neighboring neutral grain is given by[8]

$$\Gamma^s_{12}(T,\delta) \propto \int_{-\infty}^{\infty} N_1(E) N_2(E-\delta) f(E)[1 - f(E-\delta)] dE \ , \quad (10)$$

where the N's are the quasiparticle density of states of the superconducting state normalized to that of the normal state, f is the Fermi function $(1/[\exp(E/k_B T)+1])$, and δ is the change in the charging energy between two grains defined as $\delta \approx (e^2/\epsilon)(1/d_2 - 1/d_1)$, for a charge transfer from one grain to another. Here the d's are the diameters of the grains. The BCS expression

$$N(E) = \frac{1}{\sqrt{1 - [\Delta_0(T)/E]^2}} \ , \quad (11)$$

where $\Delta_0(T)$ is the superconducting energy gap at a given temperature T, is substituted into Eq. (10).

As the grains become superconducting, the charge transfer rate between the grains decreases with temperature, due to the increase in the superconducting gap Δ_0. The temperature dependence and magnetic-field dependence of the superconducting gap and the resulting changes in $N(E)$ give rise to the variation of resistance as a function of both temperature and magnetic field. Following Adkins, a Gaussian distribution for δ is assumed, i.e., $P(\delta) \propto \exp(-\delta^2/2\Delta^2)$ with the standard deviation Δ, originating from the log-normal distribution of the grain size.[8] The electrical resistance now depends on the inverse of the transfer rate, averaged over the distribution of δ, as

$$R_s(T) \propto \int_{-\infty}^{\infty} \frac{\exp(-\delta^2/2\Delta^2)}{\Gamma^s_{12}(T,\delta)} d\delta \ . \quad (12)$$

The normalized increase of resistance due to the opening of the gap in the grains is obtained from $R_s(T)/R_n(T)$, where, for the calculation of the normal-state resistance $R_n(T)$, Kim, Kim, and Lee replaced $\Gamma^s_{12}(T,\delta)$ by $\Gamma^n_{12}(T,\delta)$, for which $N_1 = N_2 = 1$ in Eq. (10).[12] As is discussed in the next section, the magnetic-field dependence of the resistivity is introduced in the BCS density of states expression by replacing $\Delta_0(T)$ with $\Delta_0(T,H)$.

D. The energy gap and critical field in small particles

Near the percolation threshold, the granular Al-Ge samples consist of a series of very small Al grains and granular clusters and the magnetoresistance is determined by the continuous suppression of the energy gap, the grains and clusters becoming normal when the gap is zero. The expression for the critical field $H_C(T)$ of a specimen where at least one dimension perpendicular to the magnetic field is less than the penetration depth, is given by (see, for instance, Fink, McLachlan, and Rothberg-Bibby[29] or Douglass[30])

$$H_C(T) = D_0 H_{CB}(T) \lambda(T)/a \ , \quad (13)$$

where $H_{CB}(T)$ is the bulk critical field, $\lambda(T)$ the penetration depth, a the radius or half thickness, and D_0 a constant which depends on the demagnetization coefficient of the entity under consideration. For instance, $D_0 = \sqrt{8}$ for a transverse cylinder and $\sqrt{20}$ for a sphere.[29] This formula shows that the grains or clusters, with the largest D_0 or the smallest a, are the last to become normal. $H_C(T)$ is well approximated, using $\lambda(T) = \lambda(0)/\sqrt{1-t^4}$ and $H_{CB}(T) = H_{CB}(0)(1-t^2)$, by[48]

$$H_C(T) = H_C(0)[(1-t^2)/(1+t^2)]^{1/2} \ , \quad (14)$$

where $t = T/T_c$ and $H_C(0) = H_{CB} D_0 \lambda(0)/a$.

To model the strong negative magnetoresistance observed in this paper, the magnetic-field-dependent energy gap $\Delta_0(T,H)$ at a fixed temperature must be taken into account. Belevtsev and Fomin[11] and Kim, Kim, and Lee[12] used Eq. (8–26) in de Gennes[31] with the assumption

$$\ln[T_c(0)/T_c(H)] = \ln[\Delta_0(0,0)/\Delta_0(0,H)] = \ln[\Delta_0(T,0)/\Delta_0(T,H)] \ .$$

In this paper the simpler expression

$$\Delta_0(T,H) = \Delta_0(T,0)\{1 - [H/H_C(T)]^2\}^n \quad (15)$$

is used in Eqs. (8), (9), and (11). Mathur, Panchapakesan, and Saxena[32] obtain $n = 1$ from a calculation based on the

BCS theory, while Ginzburg-Landau expressions all give $n=\frac{1}{2}$. Previous experimental work[30,33] gives results for n in this range. Note all the above expressions are in the approximation $a/\lambda \ll 1$. If this is not the case $[\psi(T,H)/\psi(0,H)]^2=F_0^2$, which in the Ginzburg-Landau approximation is $[\Delta_0(T,H)/\Delta_0(0,H)]^2$, can be calculated from Eq. (2.26) in Ref. 29, with $g^{1/\upsilon}$ equal to zero. The necessary diamagnetic energy terms for spheres, films, and transverse and parallel cylinders are also given in this article.

III. EXPERIMENTAL METHOD

Composite 2000-Å Al-Ge films were fabricated by coevaporating Al and Ge simultaneously using two electron guns onto room-temperature glass slices. The glass slices, cut from microscope slides, had dimensions 2.5 by 25 mm. In order to obtain the amorphous form of Ge that yields a ϕ_c of about 55% Al, it was important to maintain the substrates near room temperature.[34,35] The Ge target consisted of small chips of Ge placed into a small graphite cup.[36] The Al target consisted of a large Al semisphere melted from coiled Al wire placed in the Cu "pocket" of the second electron gun.[37] The beam of the second electron gun was concentrated onto the center of the Al target to prevent the Al from reacting with its surroundings and to prevent the Al from "spitting" and "exploding." Typical evaporation rates were 10 Å/sec for each target. Evaporation was performed in a moderately poor vacuum of 2×10^{-6} mm Hg. Twenty glass slices were glued onto an ordinary glass microscope slide which was positioned between the two targets. Thus, each slice had a different metallic Al volume fraction ϕ from its neighboring slices, with the slice closest to the Al target having the highest metallic content and the slice closest to the Ge target having the highest insulator content. About a 20% span in the Al content occurred between the two extreme slices. By varying the evaporation rates of each target, different series were obtained covering different Al concentrations. The volume fractions ϕ's were determined using an EDAX (energy dispersive analysis of x-rays) probe attached to a scanning electron microscope. Film thicknesses were measured using a depthometer and by an optical interference technique. Each film was allowed to "age" several months during which time the resistances initially increased by 10 to 30 % and then stabilized with time. Indium pads were pressed onto the ends of the Al-Ge films and copper wires were pressed onto these pads.

Transmission electron microscope studies have shown that for the insulating films with $\phi<50\%$ Al, the Al-doped germanium is amorphous.[38] In addition, the Al grains are smaller than 20 Å; in fact, they are so small that the metal can be regarded as essentially amorphous.[38] Amorphous metallic grains can exhibit enhanced superconducting transition temperatures.[1] Above the metal-insulator transition at $\phi_c \simeq 51\%$ Al, the diameter of the crystalline grains rapidly increases to 100 or 200 Å. At all except the very highest ϕ samples the Al grains are coated or partially coated with an amorphous Ge layer.[38]

Resistance measurements were performed in a He^3 adsorption refrigerator, between 4.2 and 0.45 K, which was equipped with a small superconducting magnet capable of producing a 3.5-T field perpendicular to the films. A calibrated Speer $\frac{1}{2}$ watt 470 Ω carbon resistor, which showed negligible magnetic field dependence even at 0.45 K, was used as a thermometer.[39] Resistances were measured using a Keithley 617 electrometer in its manual ranging mode, in order to control and limit the measuring current. It must be stressed that it is important to minimize internal Joule heating in these highly resistive films, even at the cost of degrading the accuracy of the resistance measurements. Resistances were all measured to an accuracy of ±5% or better. The minimum resistance that could be measured was 10 Ω corresponding to a resistivity of 10^{-5} Ω cm. It was also discovered that heating the sample holder during fast cool down to 0.45 K produced "wavylike" patterns in the R vs T data. Some of the data in Fig. 3 show this characteristic. This problem was entirely eliminated by cooling the He^3 pot down very slowly, thus avoiding the need to heat the sample holder.

IV. RESULTS AND DISCUSSION

Figure 1 shows the resistivity as a function of temperature for the no. 9 series samples, with Al concentrations between 44.4 and 51.2 vol. % Al, while Fig. 2 shows the magnetoresistivity for the same samples at 0.46 K for transverse fields up to 3.5 T. Similar results are obtained for the other series, but those for the no. 9 series best covered the range of interest. The no. 9 series has between 44.4 and 63.3 vol. % Al and its normal resistivities at 4.5 K cover 4 orders of magnitude. Somewhat similar results to those shown in Fig. 1 are given in Dynes, Garno, and Rowell[6] and White, Dynes, and Garno[7] for 2D

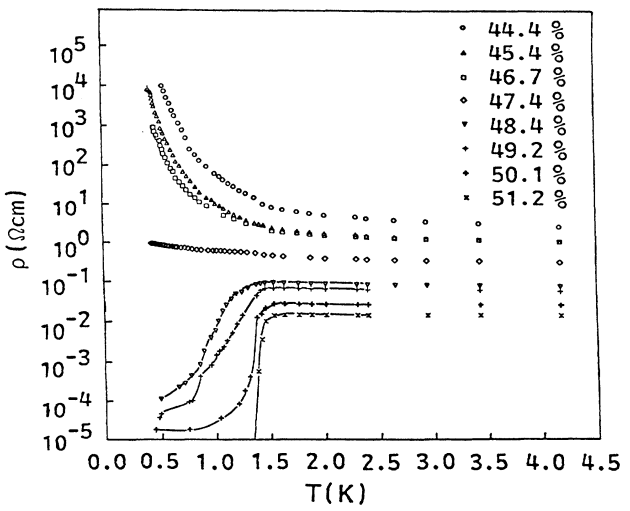

FIG. 1. A plot of the zero-field resistivity against temperature, for Al-Ge films having 44.4–51.2 vol. % Al. The lines are a guide to the eye. Note the rapid increase in the resistivity of the most insulating films at temperatures below 1.6 K.

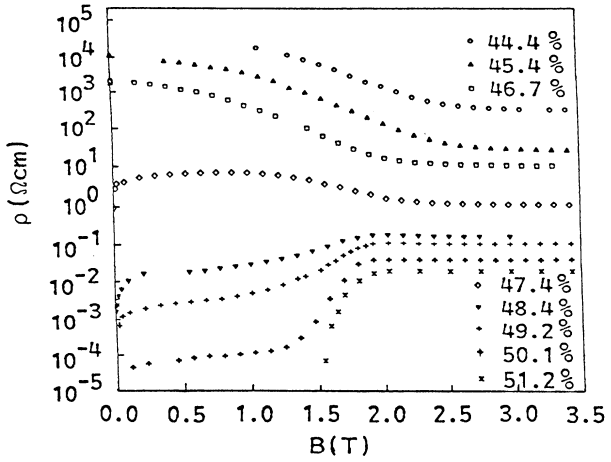

FIG. 2. A plot of the resistivity against magnetic field at 0.46 K, for the 44.4–51.2 vol. % Al specimens. The experimental value for the critical Al volume fraction $\phi_c = 50.65\%$ Al is directly deduced from this plot.

granular films, by Morozov, Naumenko, and Petinov[5] and Kunchur *et al.*[10] for 3D granular systems and by Jaeger *et al.* for ultrathin metallic films.[13]

The analysis of the resistivity and magnetoresistivity in all of these superconducting samples is made in terms of percolation theory rather than that for the dirty type-II superconductors. This is because, as Abeles argues, a normal resistivity of 2.4×10^{-3} Ω cm in Al corresponds to $k_F l \simeq 1$ (Fermi wave number times the electron mean free path) and the theory for dirty superconductors only holds for $k_F l > 1$.[1] Abeles also concludes that the resistivity of samples where $\rho \gg 2.4\times10^{-3}$ Ω cm, such as are discussed in this paper, must be due to the presence of percolation channels.[1] Furthermore, as will be shown below, the upper critical fields are relatively independent of the resistivities, which indicates weakly coupled granular materials and not type-II homogeneous superconductivity, where H_{c2} is proportional to the resistivity in the dirty limit case.[40–42] In Fig. 2, the magnetoresistance at 0.46 K is shown for the samples whose zero-field transition curves are given in Fig. 1. Following Gerber and Deutscher, we define the upper critical field of the 48.4–51.2 % and higher Al concentration samples as the point where the resistance has dropped to one-half of its normal value.[42] This criterion gives upper critical fields H_c^* starting at about 1.2 T for the 48.4% Al sample, rising to 1.7 T for the 51.2% Al sample and dropping to about 1.4 T for still higher Al concentration samples. The upper critical field is thus almost constant (1.2–1.7 T) for a change in resistivity of over 2 orders of magnitude. Following Gerber and Deutscher, if one again defines H_c^* in the more resistive insulating samples (47.4% Al and lower) as the point where the resistivity reaches its normal value in increasing fields, then Fig. 2 would indicate an H_c^* of 2.3–2.5 T for these samples.[42] However, as there is a small tail unobservable on this scale, the actual values are a little in excess of 3 T (see Fig. 5).

If one assumes the sample consists of weakly coupled grains and that these grains can still be considered as type I, as was done by Chui *et al.*, then Eq. (13) holds;[41] using $H_{CB}=0.01$ T, $\lambda=500$ Å, and a D_0 of $20^{1/2}$, then Eq. (13) predicts a radius $a \simeq 12$ Å for $H_C(0)=2$ T. One can consider the grain also as a type-II superconductor with a coherence length

$$\xi(T)=0.85[\xi_0 l T_c/(T_c-T)]^{1/2}$$

with ξ_0 (pure Al) $=16\,000$ Å and $l=2a$ and use the formula for H_c^* in the extremely weak-coupling limit for a small spherical superconductor:[40]

$$H_c^*=H_{c2}\simeq\frac{\hbar}{2e}\left(\tfrac{5}{3}\right)^{1/2}1/[a\xi(T)]\ . \tag{16}$$

Equation (16) predicts a to be 20 Å. In an Al-Al_2O_3 system with a mean radius of about 15 Å, Chui *et al.* measured an average $H_c(0)$ of about 3.6 T, in good agreement with our $H_c^*(0)=3.2$ T for $\phi \leq 47.4\%$.[41] It should, however, be noted that the upper critical field of the Al particles of this size is largely determined by the paramagnetism of the electrons.[41] The temperature dependence of H_c^* for the 51.2% Al sample, where $H_c^*(T)$ can be accurately defined and measured, follows the theoretical dependence for grains in the weak-coupling limit of $(T_c-T)^{1/2}$ better than the $(T_c-T)^{0.66}$ dependence observed experimentally by Gerber and Deutscher in random inhomogeneous Pb films.[40,42] The observed temperature dependence also closely follows Eq. (14) so the two models cannot be distinguished.

The conclusion that must be drawn from these measurements, when compared with the theories and results given in Refs. 40–42, is that the Al-Ge system consists of weakly coupled grains whose upper critical field is determined by the size of the grain (or small cluster) and not by the bulk resistivity in the case of dirty type-II superconductors. Hence, the remainder of the analysis will be done in terms of percolation theory and intergranular coupling and tunneling. Before doing this it should be noted that the radii of the grains in the 44.4–47.4 % Al samples are obviously somewhat smaller than those in the 48.4–51.2 % Al and higher Al content samples. The radii are apparently increasing with Al content at the metal-insulator transition and above which is in accord with the electron microscope observations.[38]

Near the percolation threshold, most of the Al grains are in large clusters interconnected by "strong" superconducting junctions, which go normal in fields in excess of 1.4 T as is shown by the spanning cluster in the 51.2% Al sample. In the 44.4–46.7 % Al specimens it will be shown that the clusters are coupled through quasiparticle tunneling junctions, presumably 20 Å or more thick, which determine both the resistivity and the strong negative magnetoresistivity that can be seen in Fig. 2. When the Al fraction increases, the critical junctions thicknesses fall and Josephson junctions determine the coupling between the superconducting clusters in the specimens with 48.4–50.1 % Al. As the temperature is lowered, strong superconducting fluctuations in the large

clusters are present and determine the initial drop in the resistivity above the transition temperature. Below this, the Josephson-junction coupling energies (E_J's) on the backbone percolation paths progressively rise above $k_B T$; and the resistivity continues to drop. If the lowest coupling energy E_J were to exceed $k_B T$, phase coherence would exist throughout the sample and the resistivity would drop to zero. However, we are not certain that the resistivity, even in the 50.1% Al sample, will drop to zero. The tendency seems to be to saturate to a residual value or "tail" as was observed in some of the ultrathin superconducting metallic films of Jaeger *et al.*[13] As can be seen from Fig. 2, a relatively small magnetic field ($B < 0.2$ T) destroys most of the phase coherence between the junctions which now form a random SQUID network of Josephson junctions and superconducting interconnections; and the resistivity rises rapidly for small fields. The subsequent slow return to the normal resistivity is a combination of ever diminishing phase coherence and, nearer H_c^* the quenching of superconductivity in the grains and clusters.

In the specimens with 51.2% and higher Al content, the intercluster and intracluster junctions are all strongly coupled in the sense that it takes a field in excess of 1.4 T to start to quench the superconductivity. In one model that we use, the magnetoresistance is determined by the continuous suppression of the energy gap, the grains and clusters becoming normal when the gap is zero. Here, the expression for the critical field $H_C(T)$ of a specimen, where at least one dimension perpendicular to the magnetic field is less than the penetration depth, is given by Eq. (13). Using $H_{CB}=0.01$ T, $\lambda=500$ Å, a D_0 of $(20)^{1/2}$, and a radius $a=12$ Å, Eq. (13) gives an $H_C(0)$ of 2 T. Therefore, in this model, one must assume the smallest superconducting links which form part of the percolation backbone in the 51.2% sample have transverse dimensions of the order of 20 Å. This dimension is, according to Lereah *et al.*, the size of a typical grain in the granular Al-Ge system below the percolation threshold, and somewhat below the typical dimension for $\phi \geq \phi_c$.[38]

There are several problems associated with this very small grain size. First the change in the charging energy as an electron pair tunnels from grain (r_1) to grain (r_2),

$$\Delta E_c = [2e^2/4\pi\epsilon_0][1/r_2 - 1/r_1] , \tag{17}$$

can easily be of the order of 0.1 eV ($\gg k_B T$ or E_J) at these dimensions (20 Å). It is therefore apparent that, in the type of Josephson junction that occurs near ϕ_c, the superconducting electron pairs most probably tunnel between large clusters where the capacitance of each cluster is small and $\Delta E_c < k_B T < E_J$. As discussed in Abeles,[1] superconductivity in isolated 20 Å grains is quenched as there is less than one superconducting electron per grain. Superconductivity in these grains is therefore a cooperative phenomenon between the strongly linked grains that form large superconducting clusters and the semi-isolated grains that form the links between the clusters in the 51.2% specimen.

The criterion for the critical volume fraction ϕ_c for the metal-insulator transition in McLachlan *et al.* was taken to be the presence of at least one continuous percolative backbone path in the sample, or that there is no evidence of Josephson-junction coupling on the metallic side of ϕ_c.[3] This type of behavior is shown by the 51.2% Al sample, where the very high $H_C^*(T)$ is due to the small grains and clusters on the backbone path. The criterion for the first insulating sample was taken to be the presence of Josephson junctions on the backbone, such as is shown by the 50.1% Al sample (see Figs. 1 and 2). This definition of ϕ_c requires that there be no tunnel barriers along the critical percolation or backbone path and not the more nebulous definition that the thickest junctions in the percolation path should just allow Josephson coupling at $T=0$ K. From Fig. 1 it is not clear if the 50.1% Al sample will have zero resistance at 0 K. Using the above criterion an inspection of Figs. 1 and 2 clearly shows that the metal-insulator ϕ_c lies between 50.1 and 51.2 % Al. We therefore take ϕ_c to be 50.65% Al. The metal-insulator ϕ_c defined in this way, for other series of Al-Ge samples, agrees with the ϕ_c value found from resistivity vs Al concentration results at room temperature, using a modification of the percolation equations and the general effective media (GEM) equation.[3,44,45]

However, the definition of ϕ_c for the superconductor-insulator transition must be that the amplitude of the superconducting wave function is finite at all points, along the critical paths, including in the Josephson junctions, and that there be a phase coherent state at $T=0$ in a superconducting sample. As it is not certain that the resistivity of the 50.1% sample will go to zero at 0 K and no samples exist between the 50.1 and 51.2 % samples, it is impossible to say if ϕ_c for the metal-insulator and superconductor-insulator transition are the same for the Al-Ge system.

From the resistivity (Fig. 1) and the magnetoresistivity (Fig. 2) of the 47.4% specimen it can be seen that both Josephson and quasiparticle junctions determine the resistivity and magnetoresistivity of this sample. Due to the different temperature dependence of the resistivity of Josephson and quasiparticle junctions it is, as argued by Valles and Dynes, highly improbable that any composition exists for which the resistivity is finite at absolute zero as it must be either infinite or zero at $T=0$.[43]

As the resistivity and magnetoresistivity of the samples between 44.7 and 46.7 % Al are very similar, being dominated by quasiparticle tunneling, the results for only the 45.4% Al film are discussed, and Fig. 3 shows the resistivity plotted on a logarithmic scale as a function of $1/T$ in various magnetic fields. From the curves shown in Fig. 2 it is obvious that for $B=3.45$ T the specimen is normal. The $B=3.45$ T resistivity in Fig. 3 has nearly the same slope as the zero-field line in the normal state and both closely obey the equation $\rho(T) = 0.71\exp(1.80/T)^{0.964}$. This is because the positive coefficient of magnetoresistance observed just above T_c is less than 1%, even in a field of 3.45 T. The strong magnetic field dependence of the resistivity below $T_c=1.6$ K can clearly be seen and this will be shown to be due to the magnetic field reducing the superconducting energy gap. The experimental values of $\rho(T,B)/\rho(T,3.45) \approx \rho(T,0)/\rho_n(T,0)$ are plotted against T^{-1} in Fig. 4,

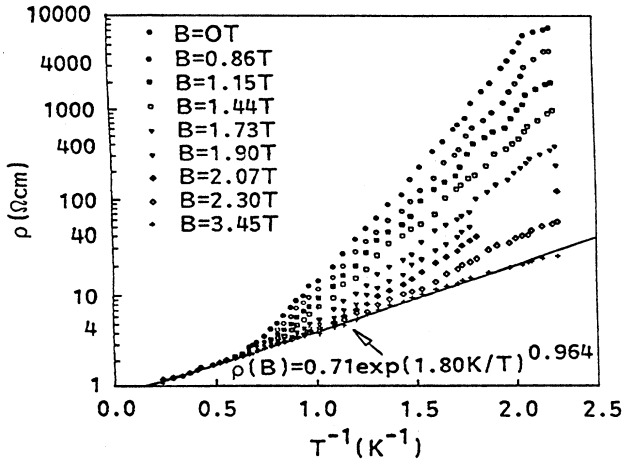

FIG. 3. A logarithmic plot of the resistivity of the 45.4% Al specimen against T^{-1} in different magnetic fields. Note the greatly enhanced values of the zero-field resistivity arising from quasiparticle (Adkins) hopping resistivity below $T_c = 1.61$ K.

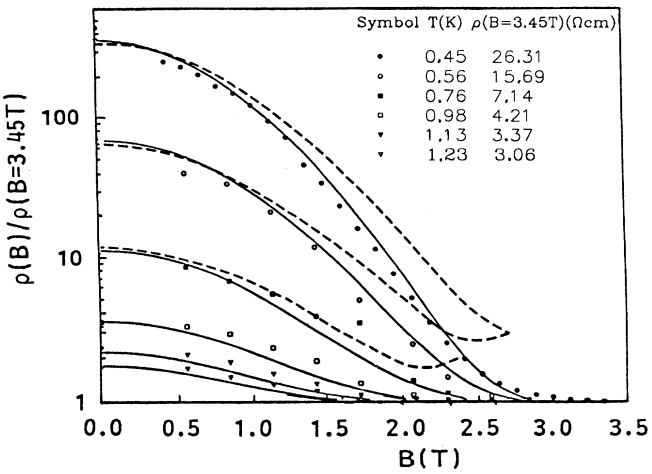

FIG. 5. A plot of the resistivity at various temperatures, normalized by the resistivity at the same temperature in a field of 3.45 T (where the sample is normal), against the magnetic field for the 45.4 vol. % Al specimen. The solid theoretical lines are from Eq. (18) and the dashed lines are obtained by inserting Eq. (15) into the BGS density-of-states expression, Eq. (11), used in the Adkins hopping model.

while in Fig. 5 the experimental values of $\rho(T,B)/\rho(T,3.45)$ are plotted against B for various temperatures. These data are unique as this is the first granular system of this nature, where the superconductivity is completely quenched. This is largely due to the low $H_C(0)$ for bulk Al of 0.01 T.

A sudden increase in the rate of the rise of the resistivity at the superconducting transition temperature for samples just on the insulating side of the superconductor-normal transition, as shown in Fig. 3, has also been observed by Morozov, Naumenko, and Petinov,[5] Dynes, Garno, and Rowell,[6] Adkins, Thomas, and Young,[8] Sin, Lindenfield, and McLean,[9] Belevtsev and Fomin,[11] White, Dynes, and Garno,[7] Kunchur *et al.*,[10] Shmuelli and Rosenbaum,[46] Gerber and Deutscher,[42,47] and Kim, Kim, and Lee.[12] In Morozov, Naumenko, and Petinov[5] and Dynes, Garno, and Rowell,[6] a small dip in the resistivity at T_c followed by the rapid rise is observed which is not the case here. Jaeger *et al.* have observed both the rapid rises and "dips" in their ultrathin granular metal films.[13]

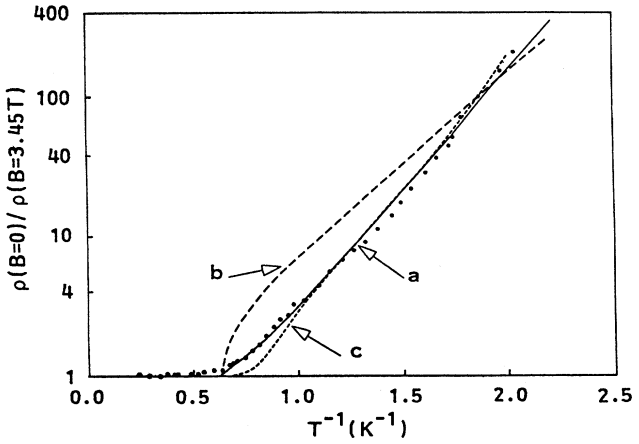

FIG. 4. A plot of the resistivity at zero field, normalized by the resistivity at the same temperature in a field of 3.45 T (where the sample is normal), against T^{-1} for the 45.4 vol. % Al. The solid theoretical line (a) is from Eq. (9), the long-dashed line (b) from Eq. (8), and the short-dashed line (c) from the Adkins hopping model discussed in the theory section. The parameters for all plots are given in the text. Note that at low temperatures, the enhanced resistivity follows a simple exponential activation law for all three theoretical models and the experimental results.

The rapid rise in resistivity illustrated in Fig. 3 was probably first clearly explained by Adkins *et al.* and has been referred to as "Adkins hopping."[8] They postulated that below the transition temperature the number of quasiparticles available to tunnel from grain (cluster) to grain (cluster) decreases with temperature due to the increasing energy gap and decreasing thermal excitation. Although this is the dominant factor in explaining the anomalous increase in the resistivity, the distribution in the differences in the charging energies [Eq. (12)], as the electron hops from one grain (cluster) to another, should also be taken into account as is discussed in Sec. II C.[8,12]

Adkins, Thomas, and Young[8] also adequately fitted the increase in their experimentally measured resistivities in the superconducting state, above those in the normal state, using the Gorter-Casimir two-fluid model, i.e., $\rho(sc)=\rho(n)(T_c/T)^4$. For the present data the best result for the two-fluid model was for $(1.37/T)^4$, which fitted the data, to within the experimental error, between 1.25 and 0.6 K. However, below this temperature the Gorter-Casimir term clearly did not have a sufficiently strong temperature dependence. See Lynton for a discussion on the Gorter-Casimir model.[48]

As the grain size is about 20 Å and there is 8 mm be-

tween the indium contact pads "an electron" must pass through a minimum of 4×10^6 junctions if all the grains were isolated by tunneling barriers. Although most of the intergranular contacts are metallic intracluster contacts, it can safely be assumed that there are 10^3-10^4 quasiparticle junctions. Therefore, as the total voltage across the sample is about 10 mV, this gives $1-10$ μV across each junction, i.e., $eV \ll k_B T$ and Δ_0, which justifies the expansion used in going from Eq. (6) to Eq. (7). In Fig. 4 the best fits to Eq. (8) [dashed line (*b*)] are with $\Delta_0(0,0)/k_B = 3.48$ K and $T_c = 1.61$ K and Eq. (9) [solid line (*a*)] with $A = 0.075$, $\Delta_0(0,0)/k_B = 3.84$ K, and $T_c = 1.61$ K are shown. In both cases the values for $\Delta_0(T,0)/\Delta_0 T(0,0)$ given by Muhlschlegel have been used.[49] For reasons which are not known, Eq. (9) gives the better fit, but with a $\Delta_0(00)/k_B T_c$ of 2.38, which is higher than the BCS value of 1.76 (see, for instance, Tinkham[50]). However, it should be noted that enhanced values of the gap to T_c values have also been observed in thin niobuim films $d \leq 50$ Å.[51] Abeles and Hanak have measured, using tunneling junctions, superconducting energy gaps of $\Delta_0(0,0)/k_B = 4.85$ K in the region where $\rho \simeq 3\times10^{-3}$ Ω cm in granular Al-SiO_2.[52] Our values for ϕ_c, ρ_c, and $\Delta_0(0,0)$ are in excellent agreement with their findings.[52]

The variation of the gap with the magnetic field at a fixed temperature, as given by Eq. (15), can be inserted into Eqs. (8) or (9) to try to arrive at an expression for magnetoresistivity results, such as those shown in Fig. 5. As Eq. (9) gave the better results in Fig. 4 and gives the best fit for the magnetoresistance, only the results based on this equation with Eq. (15) for $\Delta_0(T,H)$ and Eq. (14) for $H_C(T)$ [or $B_C(T)$] are given. The magnetoresistance equation used is therefore

$$\rho(T,B)/\rho(T,3.45) = 0.925 + 0.075 \exp\{\Delta_0(T,0)[1-H^2/H_C^2(T)]^n/k_B T\} \ . \tag{18}$$

In this equation $H_C(0)$ [or $B_C(0)$] and n are now the only free parameters as T_c, $\Delta_0(0,0)$, and $A = 0.075$ have already been determined from the zero-field data shown in Fig. 4. Better results are obtained for $n = 1$ than $n = 0.5$ and the best-fit results shown by the solid lines in Fig. 5 are for $n = 1$ and $B_C(0) = 3.19$ T. Long tails at high fields are shown both in the experimental points and the theoretical fits.

The agreement between the experimental results in Fig. 4 and the phenomenological theory given by Eq. (9) is very satisfactory. Even more remarkable is the excellent agreement obtained between this equation and the magnetoresistance results when $\Delta_0(T,H)$ is substituted for $\Delta_0(0,0)$ and the accepted field and temperature dependencies of $\Delta_0(T,H)$ and $H_C(T)$ are used. Note that only five parameters T_c, $\Delta_0(0,0)$, A, n, and $B_C(0)$ are necessary to fit all the data shown in Figs. 4 and 5 using Eqs. (9) and (18) and that none of the values for these parameters are unreasonable, except perhaps the $\Delta_0(0,0)/k_B T_c$ value of 2.38.

The normalized zero-field resistivity data shown in Fig. 4 and the magnetoresistivity data can also be fitted using the Adkins hopping model (Sec. II C). The parameters are $\Delta_0(0,0)$, which is taken to be $2.29 k_B T_c$ with $T_c = 1.61$ K, as determined from Fig. 3; Δ (which is defined in Sec. II C); and the zero-temperature critical magnetic field in Eq. (14), which is needed only for the magnetoresistivity. Δ was then varied to give a best fit to the zero-field data shown by the short-dashed line in Fig. 4. The value for Δ in this plot is $\Delta = 0.040\Delta_0(0,0)$ or 9.8 μeV, and the fit is quite acceptable. The magnetoresistivity fit, shown as dashed lines in Fig. 5, where $H_C(0)$ was fixed at the previously obtained value of 3.19 T, is not very good. Even if the parameters used could be better optimized, its basic behavior or shape does not agree with the experimental results. The fits to the resistance enhancement results shown in Fig. 4 from Eq. (9) and the Adkins model are not sufficiently different to prefer one over the other, especially as the spread in the T_c's must strongly influence the experimental results just below 1.61 K. However, as can be seen from Fig. 5, the fit to the magnetoresistance results from Eq. (18) is clearly superior to the Adkins model with a field-dependent energy gap. The small value of Δ relative to $\Delta_0(0,0)$ indicates that at the lower temperatures charging is not playing a major role, probably because the electrons are tunneling along paths determined by the larger clusters which have higher capacitance values.

Note that δ, the difference in the charging energies, appears as an integral variable and does not appear in the final results of the resistance enhancement. It should also be noted that in performing the calculation of Γ_{12}^s in Eq. (10), the integral must be broken up into regions of integration where the BCS density of states $N(E)$ and $N(E-\delta)$ are nonzero. In practice, finite integration limits for E are also used in place of the $-\infty$ and $+\infty$ that appear in Eq. (10). In order to avoid infinities arising from the BCS density of states in Eq. (11), the integration limits placed upon E are such as to allow E to closely approach the poles $-\Delta_0$, $+\Delta_0$, $\delta-\Delta_0$, and $\delta+\Delta_0$ without ever being exactly equal to them.

The conclusion of this section is that although the mechanisms leading to the phenomena observed below T_c in the 44.4, 45.4, and 46.7 % Al samples are well understood, the exact equations to describe them are not yet known. The very strong enhancement of the resistivity at very low temperatures could be used as a particle detector if the linewidth of the film is such that the energy deposited by the particle heats a finite length of the film causing it to go normal.

The last subject to be discussed is how the fitting parameters T_0 and x in the hopping resistivity equation [Eq. (4)] change as the metal-insulator transition is approached from the insulating side. Equation (4) has been fitted to the resistivity data of the insulating films in their normal state, using the procedure suggested by Zabrodskii and Zinov'eva, and the fitting parameters are summarized in Table I.[53] The temperature range of these

TABLE I. Values for the parameters appearing in the resistivity expression $\rho=\rho_0\exp(T_0/T)^x$. This expression was fitted to the normal-state resistivity data (in a magnetic field of 3.5 T) using the fitting scheme of Zabrodskii and Zinov'eva (Ref. 53).

ϕ (% Al)	T_0 (K)	x	ρ_0 (Ω cm)
50.1	0.032	0.305	0.022
49.2	0.27	0.350	0.042
48.4	0.33	0.533	0.064
47.4	0.76	0.741	0.255
46.7	1.37	0.894	0.76
45.4	1.80	0.964	0.71
44.4	2.36	1.03	1.55

fits is between 0.45 and 4.2 K. In Fig. 6, T_0 is plotted against ϕ, and in Fig. 7, the exponent x is plotted against ϕ for the no. 9 series samples with 44.4–50.1 % Al. In Fig. 7, values of x taken from samples of other more insulating series are included to show that the value of x drops to about 0.5 after peaking at about one for the samples which have been shown to be dominated by quasiparticle (Adkins) tunneling in the superconducting state. Figure 6 clearly shows that T_0 decreases very rapidly to zero at about 50% as the metal-insulator transition is approached. The 51.2% Al sample, which has already been shown to have a metallic backbone percolation path, does not obey Eq. (4) in any temperature range. The same is true in Fig. 7 which shows that the value of x drops rapidly with increasing Al content, extrapolating to zero very close to 51.2%. Therefore, both these figures allow a reasonable estimate of ϕ_c to be made, this time from measurements on the insulating side of the transition. Recall that the experimental value for ϕ_c is 50.65% Al. It should also be noted that Möbius *et al.* plotted $T_0^{1/4}$ against ϕ for the amorphous CrSi system and obtained a ϕ_c.[54]

In samples with a very small content of granular Al, the dominant resistivity is a thermally activated hopping

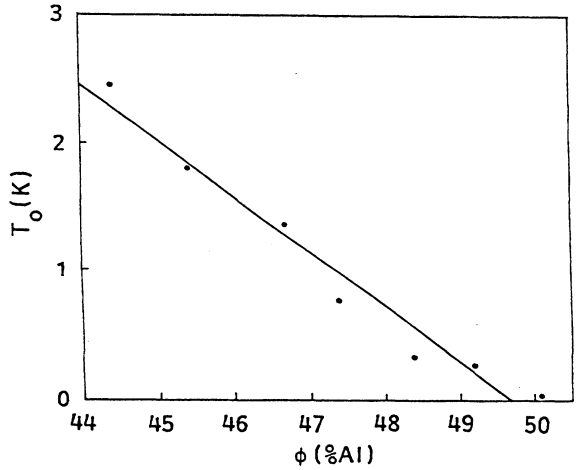

FIG. 6. A plot of the effective temperature T_0 [as defined in Eq. (4)] against ϕ, the vol. % Al. Note that extrapolating T_0 to zero yields a value for $\phi_c \simeq 49.7\%$ Al in close agreement with the experimentally observed value of 50.7% Al.

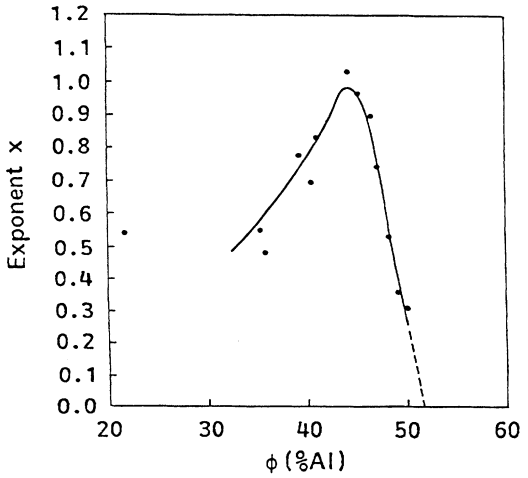

FIG. 7. A plot of the exponential x [as defined in Eq. (4)] against ϕ, the vol. % Al. By extrapolating x to zero, a value of 51.7% Al is obtained for ϕ_c in close agreement with the experimental value of 50.7% Al.

conductivity between Al sites in the Al-doped amorphous Ge component because at this state the intersite distance of the Al-dopant sites in the Ge is much less than the distance between the Al grains. This is probably true for $\phi<0.35$ where x is found to be about 0.5. As the intergranular distance decreases with increasing Al content, intergranular tunneling becomes possible and eventually a mixture of site and granular hopping prevails. This situation would appear to occur for samples with $0.35<\phi<0.45$. As the exponent x peaks at a value of around one, the intergranular or intercluster hopping conductivity must be closer to nearest-neighbor hopping, as envisaged in the Neugebauer-Webb model ($x=1$), than any of the other models mentioned in the theory section.[14] The rapid decrease in T_0 or alternatively E_c^0 in Eq. (2), above 44.4% is probably due to a very rapid increase in the Al cluster sizes, between which tunneling is taking place, as the percolation threshold is approached. This leads to a rapidly increasing effect "d" in Eq. (2) and a correspondingly rapid decrease in E_c^0 or T_0. There is no obvious explanation for the corresponding drop in x, other than that the intergranular tunneling must become less important as ϕ_c is approached, being completely short circuited out above ϕ_c (as evidenced by magnetoresistance measurements in the superconducting state).

V. SUMMARY AND CONCLUSIONS

The work presented in this paper is a complete investigation of the metal-insulator and superconductor-insulator transition in the granular Ge-Al system. The investigation, using both resistivity and magnetoresistivity measurements close to ϕ_c at temperatures between 0.46 and 4.2 K has clearly identified three distinct regions, all of which are understood in a qualitative way. Whether exact theories for all the phenomena observed in granular Al-Ge near ϕ_c will ever be available is doubtful, due to the complexity of the structure near ϕ_c, and the number of different conduction processes occurring

simultaneously.

On the conducting side of ϕ_c, superconductivity measurements show the existence of metallically linked percolation backbones. The high critical field in the superconducting state clearly shows that crucial links in the backbone consists of a series of strongly coupled fine grains (20 Å) and/or small granular clusters. No exact analysis can be attempted due to the complexity and lack of knowledge of the microstructure of the system; but it is obvious that superconducting fluctuations are playing a major role in determining the shape of the transition.[55–57] McLachlan *et al.* have shown that normal-state samples with ϕ just greater than ϕ_c have a negative temperature coefficient of resistivity.[3] This is due to a weak or strong electron-electron interaction and to weak or strong localization effects in the "fine wire" metallic backbone.

On the insulating side of ϕ_c, it is apparent that the resistivity (and magnetoresistivity) is first dominated by superconducting fluctuation conductivity in the large clusters joined by Josephson junctions; these form the conduction paths of the system. The distribution of the junctions along the backbones and the spread in the coupling energies determines the low-temperature behavior of the zero-field resistivity curve. The low-field magnetoresistance is determined by the distribution of the Josephson junctions on the random netlike conduction paths and the area (perpendicular to the field) contained in each loop of the net—these form a multiple SQUID-type structure. Again a quantitative analysis is not possible.

When $4\% \leq (\phi_c - \phi) \leq 7\%$ and many of the tunnel barriers on the percolating networks are too thick for tunneling by Cooper pairs, quasiparticle tunneling between the grains and clusters or Adkins hopping conductivity dominates the resistivity. This manifests itself as a rapid increase in the resistivity with decreasing temperature below T_c and a spectacular negative magnetoresistivity. These phenomena are due to the variation in the number of quasiparticles available to tunnel between the grains and clusters, the number being determined by the temperature and the size of the gap, which is, in turn, dependent on the temperature and magnetic field. Various equations, two of which are based on these concepts, were used to try to fit the experimental resistivity and magnetoresistivity results. Unfortunately, the best fits for both types of data were obtained with purely phenomenological equations [Eqs. (9) and (18)], which implies that more theoretical work needs to be done in this area.

One serious problem has not been addressed so far. When the grains are so small and the grains are weakly coupled, the thermodynamic fluctuations will broaden the superconducting transition to a point where a discontinuity in the specific heat will not be observed.[58,59] The critical grain length at which this is observed is given by $L_c = \{1/[N(0)k_B T_c]\}^{1/3}$, where $N(0)$ is the density of states; a typical value for L_c is 30 Å.[60,61] As L_c^3 is also the volume occupied by one Cooper pair, it is obvious that fluctuations can wash out the superconducting transition in an isolated grain and that these fluctuations can only be completely quenched when the grain is part of an infinite cluster. In a large cluster the fluctuations are suppressed. This again supports an earlier contention that the quasiparticle and pair tunneling is occurring between large clusters. The characteristic dimension of the cluster is given by $\xi_P \simeq 2a/(\phi_c - \phi)^{0.85}$, where ξ_P is the percolation correlation length.[62] The number of grains in a cluster is therefore of the order of $[1/(\phi_c - \phi)^{0.85}]^3/2$ or about 10^3 for the 45.4% film. With this number of grains, superconductivity must be occurring.

Lastly, it was shown that ϕ_c could also be obtained from careful measurements of the low-temperature normal-state resistivity on the insulating side of ϕ_c, in a magnetic field if necessary. These resistivity results are then fitted to the general hopping conductivity equation [Eq. (4)] and the temperatures T_0 and the exponents x determined. When T_0 and x are plotted against ϕ, the extrapolations to 0 are close to ϕ_c for T_0 and very close to ϕ_c for x. Unfortunately, both of these observations are at this state purely empirical.

The metal-insulator transition in the granular Al-Ge system has been extensively and profitably studied from many years both at room and low temperatures.[2] However, there has always been some difficulty in identifying the exact metal-insulator composition ϕ_c for the percolation threshold, at which the metal-insulator transition takes place, due to the finite resistivities of both components. Therefore, one of the most important aspects of this work has been to show how the metal-insulator and superconductor-insulator composition can be unambiguously identified by measurements in the superconducting state. McLachlan *et al.* have shown that the ϕ_c obtained in this way agrees with that obtained by fitting the general effective media theory and percolation theory (taking into account the concept of a crossover region) to resistivity results obtained at room temperature.[3]

ACKNOWLEDGMENTS

The authors gratefully acknowledge the help and guidance of University of the Witwatersrand's Electron Microscope Unit in making the EDAX measurements. We are also indebted to N. Grammatica for her assistance in doing the EDAX analysis of these samples and to Dr. M. Witcomb. We greatly thank Dr. Yoad Yagil for preparing the samples. We thank G. Deutscher for valuable discussions. We are grateful to the Israeli Ministry of Science and Technology for financial support for D.M.

[1]B. Abeles, in *Applied Solid State Science,* edited by R. Wolfe (Academic, New York, 1976), Vol. 6, p. 1.

[2]G. Deutscher, A. Kapitulnik, and M. Rappaport, in *Percolation Structures and Processes,* edited by G. Deutscher, R. Zallen, and Joan Adler (Annals of Israeli Physical Society, Jerusalem, 1983), Vol. 5, p. 207.

[3]D. S. McLachlan, R. Rosenbaum, A. Albers, G. Eytan, N. Grammatica, G. Hurvits, J. Pickup, and E. Zaken, J. Phys. C (to be published).

[4]G. Hurvits, R. Rosenbaum, and D. S. McLachlan J. Appl.

Phys. **73**, 7441 (1993).
[5]Yu. G. Morozov, I. G. Naumenko, and V. I. Petinov, Fiz. Nizk. Temp. **2**, 987 (1976) [Sov. J. Low. Temp. Phys. **8**, 484 (1976)].
[6]D. C. Dynes, J. P. Garno, and J. M. Rowell, Phys. Rev. Lett. **40**, 479 (1978).
[7]Alice E. White, R. C. Dynes, and J. P. Garno, Phys. Rev. B **33**, 3549 (1986).
[8]C. J. Adkins, J. M. D. Thomas, and M. W. Young, J. Phys. C **21**, 3427 (1980).
[9]H. K. Sin, P. Lindenfeld, and W. L. McLean, Phys. Rev. B **30**, 4067 (1984).
[10]M. Kunchur, Y. Z. Zhang, P. Lindenfeld, and W. L. McLean, Phys. Rev. B **36**, 4062 (1987).
[11]B. I. Belevtsev and A. V. Fomin, Fiz. Nizk. Temp. **12**, 103 (1986) [Sov. J. Low Temp. Phys. **12**, 60 (1986)]; B. I. Belevtsev, Yu. F. Komnik, and A. V. Fomin, *ibid.* **12**, 821 (1986) [*ibid.* **12**, 465 (1986)].
[12]Ju-Jin Kim, Jinhee Kim, and Hu Long Lee, Phys. Rev. B **46**, 709 (1992).
[13]H. M. Jaeger, D. B. Haviland, B. G. Orr, and A. M. Goldman, Phys. Rev. B **40**, 182 (1989).
[14]C. A. Neugebauer and M. B. Webb, J. Appl. Phys. **33**, 74 (1962).
[15]P. Sheng, B. Abeles, and Y. Arie, Phys. Rev. Lett. **31**, 44 (1973).
[16]C. J. Adkins, J. Phys. C **15**, 7143 (1982).
[17]N. F. Mott, J. Non-Crystal Solids **1**, 1 (1968).
[18]C. J. Adkins, in *Hopping and Related Phenomena,* edited by H. Fritzche and M. Pollak (World Scientific, Singapore, 1990), p. 97.
[19]A. L. Efros and B. I. Shklovskii, J. Phys. C **8**, L49 (1975).
[20]C. J. Adkins, J. Phys. Condens. Matter **1**, 1253 (1989).
[21]Ping Sheng, Philos. Mag. B **65**, 357 (1992).
[22]A. L. Efros and B. I. Shklovskii, Phys. Status Solidi B **76**, 475 (1976).
[23]Y. Imry, Y. Gefen, and D. J. Bergman, Phys. Rev. B **26**, 3436 (1982).
[24]D. S. McLachlan, Solid State Commun. **72**, 831 (1989).
[25]D. S. McLachlan, A. Priou, I. Chenerie, E. Isaac, and F. Henry, J. Electromagn. Waves Applic. **6**, 1099 (1992).
[26]D. H. Douglass, Jr. and L. M. Falicov, in *Progress in Low Temperature Physics,* edited by C. J. Gorter (North-Holland, Amsterdam, 1964), Vol. IV.
[27]T. van Duzer and C. W. Turner, *Principles of Superconductive Devices and Circuits* (Elsevier, New York, 1981), p. 87.
[28]*Handbook of Mathematical Functions, with Formulas, Graphs, and Mathematical Tables,* edited by M. Abramowitz and I. Stegun (U.S. GPO, Washington, D.C., 1964), p. 378.
[29]H. Fink, D. S. McLachlan, and B. Rotherg-Bibby, in *Progress in Low Temperature Physics,* edited by D. F. Brewer (North-Holland, Amsterdam, 1978), Vol. VII B, p. 435.
[30]D. H. Douglass, Jr., Phys. Rev. Lett. **6**, 346 (1961).
[31]P. G. de Gennes, *Superconductivity of Metals and Alloys* (Benjamin, New York, 1966).
[32]V. S. Mathur, N. Panchapakesan, and R. P. Saxena, Phys. Rev. Lett. **9**, 374 (1962).
[33]D. E. Morris and M. Tinkham, Phys. Rev. **134**, A1154 (1964).
[34]A. Kapitulnik, M. Rappaport, and G. Deutscher, J. Phys. Lett. **42**, L541 (1981).
[35]G. Deutscher and Y. Lereah, Physica A **140**, 191 (1986).
[36]Germanium metal $\frac{1}{4}''$ pieces of 99.999+% purity: Cerac, Inc., 407 North 13th St., Milwaukee, WI 53233.
[37]Aluminum wire MARZ grade 99.999% purity: Material Research Corp., Route 303, Orangeburg, NY 10962.
[38]Y. Lereah, G. Deutscher, and E. Grunbaum, Phys. Rev. A **44**, 8316 (1991); Y. Lereah (private communication).
[39]W. C. Black, W. R. Roach, and J. C. Wheatley, Rev. Sci. Instrum. **35**, 587 (1964).
[40]G. Deutscher, O. Entin-Wohlman, and Y. Shapira, Phys. Rev. B **22**, 4264 (1980).
[41]T. Chui, P. Lindenfeld, W. L. McLean, and K. Mui, Phys. Rev. B **24**, 6728 (1981).
[42]A. Gerber and G. Deutscher, Phys. Rev. Lett. **63**, 1184 (1989).
[43]J. M. Valles and R. C. Dynes, in *Physical Phenomena in Granular Materials,* edited by G. D. Cody, T. H. Geballe, and P. Sheng, MRS Symposia Proceedings No. 195 (Materials Research Society, Pittsburgh, 1990).
[44]D. S. McLachlan, J. Phys. C **20**, 865 (1987).
[45]D. S. McLachlan, M. Blaszkiewics, and R. E. Newnham, J. Am. Ceram. Soc. **73**, 2187 (1990).
[46]H. Schmuelli and R. Rosenbaum, Physica B **169**, 489 (1991).
[47]A. Gerber, J. Phys. Condens. Matter **2**, 8161 (1990).
[48]E. A. Lynton, *Superconductivity* (Methuen, London, 1969), p. 20.
[49]B. Muhlschlegel, Z. Phys. **155**, 313 (1959).
[50]M. Tinkham, *Introduction to Superconductivity* (McGraw-Hill-Kogakusha, Tokyo, 1975), p. 34.
[51]J. W. P. Hsu and A. Kapitulnik, Phys. Rev. B **45**, 4819 (1992).
[52]B. Abeles and J. J. Hanak, Phys. Lett. **34A**, 165 (1971).
[53]A. G. Zabrodskii and K. N. Zinov'eva, Zh. Eksp. Teor. Fiz. **86**, 727 (1984) [Sov. Phys. JETP **59**, 425 (1984)].
[54]A. Mobius, H. Vinzelberg, C. Gladun, A. Heinrich, D. Elefant, J. Schumann, and G. Zies, J. Phys. C **18**, 3337 (1985).
[55]L. G. Aslamazov and A. I. Larkin, Fiz. Tverd. Tela **10**, 1104 (1968) [Sov. Phys. Solid State **4**, 875 (1968)].
[56]K. Maki, Prog. Theor. Phys. **40**, 193 (1968).
[57]R. S. Thompson, Phys. Rev. B **1**, 327 (1970).
[58]R. L. Filler, P. Lindenfeld, T. Worthington, and G. Deutscher, Phys. Rev. B **21**, 5031 (1980).
[59]G. Deutscher, O. Entin-Wohlman, S Fishman, and Y. Shapira, Phys. Rev. B **21**, 5041 (1980).
[60]G. Deutscher, Y. Imry, and L. Gunther, Phys. Rev. B **10**, 4598 (1974).
[61]Y. Imry and M. Strongin, Phys. Rev. B **24**, 6353 (1981).
[62]D. Stauffer, *Introduction to Percolation Theory* (Taylor and Francis, London, 1985).